Acta Oncologica, 2013; 52: 1730–1738

informa
healthcare

ORIGINAL ARTICLE

Peritoneal macrophages mediated delivery of chitosan/siRNA nanoparticle to the lesion site in a murine radiation-induced fibrosis model

ISABEL NAWROTH[1,2,3], JAN ALSNER[3], BENT W. DELEURAN[4], FREDERIK DAGNAES-HANSEN[4], CHUANXU YANG[1,2], MICHAEL R. HORSMAN[3], JENS OVERGAARD[3], KENNETH A. HOWARD[1,2], JØRGEN KJEMS[1,2] & SHAN GAO[1,2]

[1]*Interdisciplinary Nanoscience Center (iNANO), Aarhus University, Aarhus C, Denmark,* [2]*Department of Molecular Biology and Genetics, Aarhus University, Aarhus C, Denmark,* [3]*Department of Experimental Clinical Oncology, Aarhus University Hospital, Aarhus C, Denmark and* [4]*Department of Biomedicine, Aarhus University, Aarhus C, Denmark*

Abstract

Background. Radiation-induced fibrosis (RIF) is a dose-limiting complication of cancer radiotherapy and causes serious problems, i.e. restricted tissue flexibility, pain, ulceration or necrosis. Recently, we have successfully treated RIF in a mouse model by intraperitoneal administration of chitosan/siRNA nanoparticles directed towards silencing TNF alpha in local macrophage populations, but the mechanism for the therapeutic effect at the lesion site remains unclear. *Methods.* Using the same murine RIF model we utilized an optical imaging technique and fluorescence microscopy to investigate the uptake of chitosan/fluorescently labeled siRNA nanoparticles by peritoneal macrophages and their subsequent migration to the inflamed tissue in the RIF model. *Results.* We observed strong accumulation of the fluorescent signal in the lesion site of the irradiated leg up to 24 hours using the optical imaging system. We further confirm by immunohistochemical staining that Cy3 labeled siRNA resides in macrophages of the irradiated leg. *Conclusion.* We provide a proof-of-concept for host macrophage trafficking towards the inflamed region in a murine RIF model, which thereby suggests that the chitosan/siRNA nanoparticle may constitute a general treatment for inflammatory diseases using the natural homing potential of macrophages to inflammatory sites.

Recruitment of macrophages to inflamed sites is a consequence of the inflammatory process that can lead to either initiation of tissue repair or promote the inflammatory events that eventually can lead to fibrosis. Classically, macrophage activation will lead to the presentation of antigens, interaction with other immune cells, and phagocytosis of foreign particles or microbes accompanied with the production of various cytokines and growth factors [1]. There is, therefore, good rational to focus on macrophages as a potential cellular target for anti-inflammatory treatment by inhibiting the production of cytokines and growth factors. Based on the pivotal role of the cytokine TNFα during inflammation and the ability for chitosan/TNFα-specific siRNA nanoparticle to silence TNFα in macrophages [2], we and others have successfully prevented murine radiation-induced fibrosis (RIF) [3] and rheumatoid arthritis [4,5] after intraperitoneal administration of chitosan/TNFα-siRNA nanoparticle. We hypothesize that the nanoparticles are phagocytosed and enter local peritoneal macrophages, which subsequently undergo systemic migration and recruitment to inflamed regions where they exhibit reduced production of TNFα. However, we have no direct experimental evidence for this recruitment mechanism from our previous studies.

Visualization of macrophage migration has a high relevance for both diagnostic purposes and the evaluation of therapeutic interventions. Tracking of migrating macrophages has been conducted in several animal

Correspondence: S. Gao, Department of Molecular Biology and Genetics, Aarhus University, C. F. Møllers Alle, Building 1130, 8000 Aarhus C, Denmark. Tel: +45 87154975. Fax: +45 86196500. E-mail: shg@mb.au.dk

(Received 4 April 2012; accepted 24 August 2012)

ISSN 0284-186X print/ISSN 1651-226X online © 2013 Informa Healthcare
DOI: 10.3109/0284186X.2012.726373

disease models using non-invasive techniques such as magnetic resonance imaging (MRI) [1], positron emission tomography (PET) [6], molecular-genetic imaging [7], optical fluorescence imaging and scintigraphy [8]. These studies involve ex vivo manipulation or genetically modified primary macrophages or the injection of cell lines into the animal followed by fluorescent monitoring. However, these results may be influenced by cell damage and toxicity from labeled compounds. It therefore remains an interesting study to monitor host macrophage trafficking and to understand its interaction with other immune cells during inflammation.

Radiation-induced fibrosis (RIF) is a common late side effect of radiotherapeutic cancer treatment. A RIF model in mice has been established that closely resembles the clinical appearances in humans [3,9]. Using this model, we applied two imaging techniques to investigate the uptake of chitosan/siRNA nanoparticles by peritoneal macrophages after intraperitoneal administration and the subsequent distribution of the fluorescent labeled siRNA to the RIF site in the hind leg.

Firstly, the optical fluorescence imaging was used to track the siRNA Cy5 fluorescent signal after intraperitoneal injection of chitosan/siRNA nanoparticles. A fluorescent siRNA signal was only observed in the footpad up to 24 hours post-injection that had been irradiated with 45 Gy 13 days before imaging, but was absent in both non-irradiated leg in the same mouse or in control mice not irradiated. Secondly, histological examination was performed to evaluate the location of chitosan/Cy3 labeled siRNA in the tissue. We only detected a Cy3 siRNA signal at the inflamed site within the leg that had been irradiated with 45 Gy, and a histological examination revealed that the siRNA was co-localized within macrophages. This provides strong evidence that host macrophages containing nanoparticles home towards the inflamed region in a murine RIF model.

Material and methods

Chitosan/fluorescent labeled-siRNA nanoparticles

siRNA-EGFP was synthesized with 2-nucleotide LNA overhangs at the 3′ ends and HPLC-purified by Ribotask, Odense, Denmark. Duplexes with Cy5 fluorescence labeled sense strand or Cy3 labeled antisense strand (location within the sequence was indicated below) were applied for whole animal optical imaging and fluorescence microscopy study, respectively. Sequences are: EGFP duplex with Cy5 labeled sense strand, SS 5′-Cy5-GACGUAAACGG CCACAAGU**TC**-3′ and AS 5′-ACUUGUGG CCGUUUACGUC**GC**-3′; EGFP duplex with Cy3 antisense strand, SS 5′–GACGUAAACGGCC ACAAGU**TC-**3′ and AS 5′-ACUUGUGGCCGU UUACGUC**G**Cy3**C**U-3′. LNA modification is indicated in bold.

Chitosan was supplied from Novamatrix (Norway) and further deacetylated with 47.7% NaOH at 60°C for 24 hours (the degree of deacetylation is >98% and the molecular weight is 190 kDa). Chitosan was dissolved in sodium acetate buffer (0.2 M NaAc, pH 4.5) to obtain a 1 mg/ml solution and then adjusted to pH 5.5 by adding 300 mM NaOH. Twenty microliters of siRNA (100 μM) in nuclease-free water was added to 1 ml of filtered chitosan (1 mg/ml) whilst stirring for one hour. Nanoparticles formed at ~N:P 60 were used in all experiments.

In vivo fluorescence imaging in a murine RIF model

Two independent experiments were performed using male C3D2F1 mice (C3H/HeJTac x_DBA/2JTac, Taconic Europe, Ry, Denmark) for the present study. For the first, the right hind leg/paw was irradiated with a single dose of 45 Gy either 13, eight, four days or one day before imaging, and a control group without irradiation was also included (n = 2 for each group). For the second, the right hind leg/paw was irradiated with a single dose of 45 Gy 13 days before imaging and a control group without irradiation was included as well (n = 5 for each group). All procedures of animal work were approved by 'The Experimental Animal Inspectorate in Denmark' under The Danish Veterinary and Food Administration, Ministry of Food, Agriculture and Fisheries (Registration number: 2010/561-1929-C3, issue date: February 28, 2011). The animals were provided with painkillers during the acute phase (from day 9 after irradiation) of the lesion by adding buprenorphine to the drinking water (Temgesic®, Reckitt Benckiser Healthcare, England) at a dose corresponding to 0.7–1.4 mg/kg.

Hair from the hind legs and the abdomen was removed by shaving to avoid autofluorescence during imaging. A single dose of 200 μl chitosan/Cy5 labeled siRNA (containing 10 μg siRNA duplex, equal to ~0.4 mg/kg) nanoparticles was injected into the peritoneum. The mice were scanned using an IVIS® 200 imaging system (Xenogen, Caliper Life Sciences) under anesthesia with 2.5% isoflurane. Cy5 excitation (λex = 640 nm) and emission (λem = 700 nm) filters were used. Identical illumination settings, including exposure time (1 second), binning factor (medium), f-stop (1), and fields of view (25 × 25 cm), were used for all image acquisitions. Total emission from inflicted areas (Region of Interest, ROI) of each mouse was quantified using Living Image 4.0 software package. According to the user instruction, the radiant efficiency of footpad was measured

(photons/s/cm^2/sr)/ (μW/cm^2), which is presented radiance/illumination power density. Background fluorescence was subtracted prior to analysis.

Fluorescence microscopy

The right hind leg of male C3D2F1 mice was irradiated with a single dose of 45 Gy whereas the left hind leg received no irradiation (n = 4). After 13 days, a single dose of 200 μl chitosan/Cy3 labeled siRNA nanoparticles was intraperitoneally injected. Mice were sacrificed four hours post-injection and skin biopsies from both irradiated and non-irradiated legs were taken. Tissue samples were preserved either in 4% formalin or embedded in Tissue Tek®, DAPI stained and visualized by confocal microscopy.

Immunohistochemical (IHC) macrophage staining

RIF tissue sections were taken to investigate the tissue and cellular location of the siRNA signal. Formalin-fixed, paraffin embedded skin biopsies were cut into 2 μm sections using a Microm HM 360 microtome (Microm, Walldorf, Germany). The sections were placed on superfrost + slides, deparaffinized in xylene and rehydrated in an ethanol gradient, followed by blocking in PBS/BSA. Sections were incubated for two hours with the primary anti-mouse F4/80 antibody (1:100, Abcam, Copenhagen) and then incubated for two hours with the secondary anti-rat antibody (daylight 649) (1:100, Jackson Immuno Research). Finally the sections were embedded in Duolink II mounting medium with Dapi (OLink Bioscience). Images of representative fields were acquired using the 488 nm line of a multiline argon laser, the 543 nm line of the green heliumneon laser, and the 633 nm line of the heliumneon laser on a confocal laser scanning microscope (LSM710; Zeiss, Jena, Germany) with a 63× oil-immersion objective.

Statistical analysis

Student's t-test was performed to evaluate the significant difference for the quantity of fluorescence signal between two sides of footpads – irradiated and non-irradiated.

Results

Assessment of acute skin reaction

Mice were subjected to 45 Gy irradiation to a limited section of the right hind limb, which has previously been determined as the dose that causes severe fibrosis (starting after 40 days in average and after six months all mice generally have developed fibrosis). The effect of irradiation was assessed for the skin phenotype following the procedures for fibrosis assessment and scoring previously described [3].

No differences for the skin could be observed among the control mice and mice irradiated eight days, four days or one day before scoring. In contrast, mice irradiated 13 days before scoring showed a strong acute skin reaction compared to the control. The mice exhibited an acute skin grade of 3.0 (moist desquamation of 75% of skin area, foot shapeless, one or two toes can be identified) or higher. This result was in agreement to our previous finding that acute skin reactions were first observed at day 10 after irradiation [3].

In vivo optical fluorescence imaging analysis

All mice were shaved before chitosan/Cy5 labeled siRNA nanoparticles were intraperitoneally (i.p.) injected. Subsequently the mice were dorsally and ventrally imaged at distinct time points. While ventrally imaged, there was slight autofluoresence signal in peritoneal cavity region before injection (Figure 1A). The specific fluorescent signal in the injection region was clearly seen after injection and peaked at one hour post-injection as 5.3-fold higher than before injection (Figure 1B), then gradually decreased during 24 hour period down to ~25% of the level at one hour (Figure 1C).

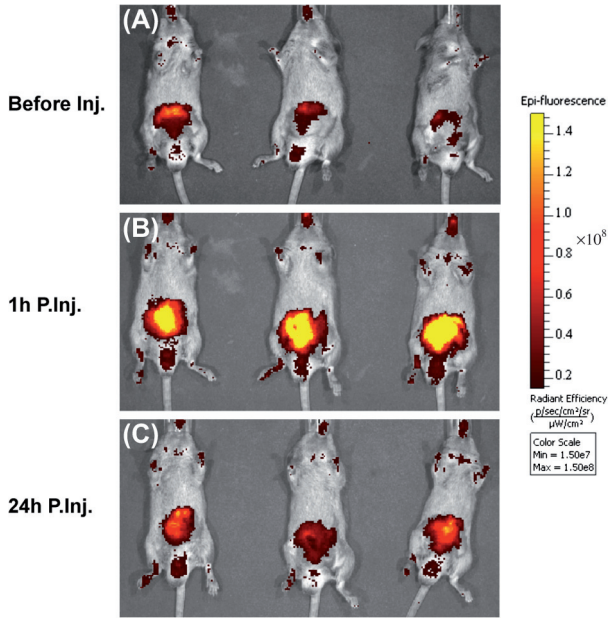

Figure 1. Altered fluorescent intensity in peritoneal cavity during 24 hour period. Mice from both control and irradiated groups were ventrally scanned before and after injection i.p. of chitosan/Cy5-siRNA. Only irradiated mice are presented. (A), before injection (Before Inj.); (B), 1 hour post-injection (1 h P.Inj.) and (C) 24 hour period (24 h P.Inj.).

The subsequent images were all dorsally scanned to place legs/paws in a convenient position for a better demonstration of the signal from the footpads.

We performed our first experiment to investigate chitosan/Cy5-siRNA nanoparticle trafficking in mice irradiated 13, eight, four days or one day before imaging or control mice without any irradiation. No specific Cy5 signal was detected in control mice and in mice irradiated eight, four days or one day before imaging at all-time points. However, a significantly enhanced Cy5 signal was detected one hour post-administration at the inflamed site of the right hind footpad of mice irradiated 13 days before imaging and lasted up to four hours (data not shown).

Therefore, we repeated the experiment but included only mice irradiated 13 days before imaging and control mice without irradiation. The imaging was performed before and right after i.p. injection of chitosan/Cy5siRNA nanoparticles, as well as at one, two, four, six and 24 hours post-injection. Similarly to the former experiment, there was no specific signal in both hind footpads in mice without irradiation (Figure 2A, C, E, G, I, K and M), and in the left hind footpads (non-irradiated side) in irradiated mice (Figure 2B, D, F, H, J, L and N). No specific signal was detected in the irradiated footpads (right side) of irradiated mice before and right after i.p. injection (Figure 2B and D). However, a clearly enhanced Cy5 signal was detected one hour post-administration at the inflamed site of the right hind footpad (Figure 2F) compared to the non-irradiated left hind footpad of the same mice as well as both hind footpads of the control mice (Figure 2E). The signal was further enhanced from two to four hours post-administration (Figure 2H and J) and for some mice even further at six hours post-administration (Figure 2L). The signal was still detectable at 24 hours post-administration (Figure 2N). To quantify the intensity of the fluorescent signal, the radiant efficiency [(photons/s/cm^2/sr)/(μW/cm^2)] was measured for both sides of hind footpads from mice with or without irradiation. The fluorescent signal was also slightly increased from one to four/six hours post-injection in non-irradiated footpads, which probably was contributed by circulating chitosan/Cy5 siRNA in the bloodstream. However, a significant difference was found between the signal from the irradiated side and control side at all time-points from one hour to 24 hours, evaluated by Student t-test ($p < 0.05$ or $p < 0.01$) (Figure 3).

The observation suggests that only mice irradiated 13 days before imaging showed a strong acute skin reaction and the specific Cy5 signal was only present in the inflammatory site, indicating a correlation between nanoparticle accumulation and radiation induced inflammation.

Co-localization of chitosan/Cy3 labeled siRNA and peritoneal macrophages at the irradiation site

Using optical imaging we were able to visualize in real time the trafficking of chitosan/Cy5 labeled siRNA nanoparticles into the irradiated region. However, it is difficult to assess whether the particles migrate to the site of inflammation via the macrophages or as free particles. Therefore, we performed histological examination experiments. Based on the results obtained from the optical imaging, we limited the study to include the group irradiated 13 days with a dose of 45 Gy and the non-radiated control group. We injected i.p. chitosan/Cy3 labeled siRNA nanoparticles for these two groups of mice. Mice were sacrificed four hours post-injection, and skin biopsies from the irradiated and non-irradiated hind leg were taken. Both formalin fixed, paraffin-embedded tissue sections and frozen tissue sections were evaluated by fluorescent confocal microscopy. Classical HE staining was performed first and typical features for inflammation were observed in samples from irradiated skin (Supplementary Figure 1, available online at http://informahealthcare.com/doi/abs/10.3109/0284186X.2012.726373).

Under fluorescent confocal microscopy a Cy3-siRNA signal was clearly detected in the cytoplasm of a cellular population of 45 Gy irradiated skin samples. The cells appeared to be monocytes or macrophages based on their morphology, with enlarged nuclei and irregular shape and positive for the macrophage marker F4/80 (Figure 4A–D), indicating that the chitosan/Cy3-siRNA nanoparticles exclusively resided within macrophages. No signal was observed in the samples from control tissues (Figure 4E and F).

Discussion

Our in vivo imaging study suggests that fluorescently labeled siRNA/chitosan nanoparticles are taken up by murine peritoneal macrophages and transported to the irradiated site. This was further demonstrated by histological examination and immunohistochemical staining. The data confirm the hypothesis in our previous studies that the therapeutic effect, obtained by intraperitoneal delivery of chitosan/DsiRNA nanoparticles targeting TNF alpha, is due to macrophage recruitment at the sites with radiation-induced fibrosis [3], a mechanism that presumably also occurs in the case of rheumatoid arthritis in mice [4].

To detect macrophage trafficking and to understand cellular interactions during inflammation, the application of optical imaging systems becomes more important and relevant. Two alternate strategies that have previously been used are direct labeling or

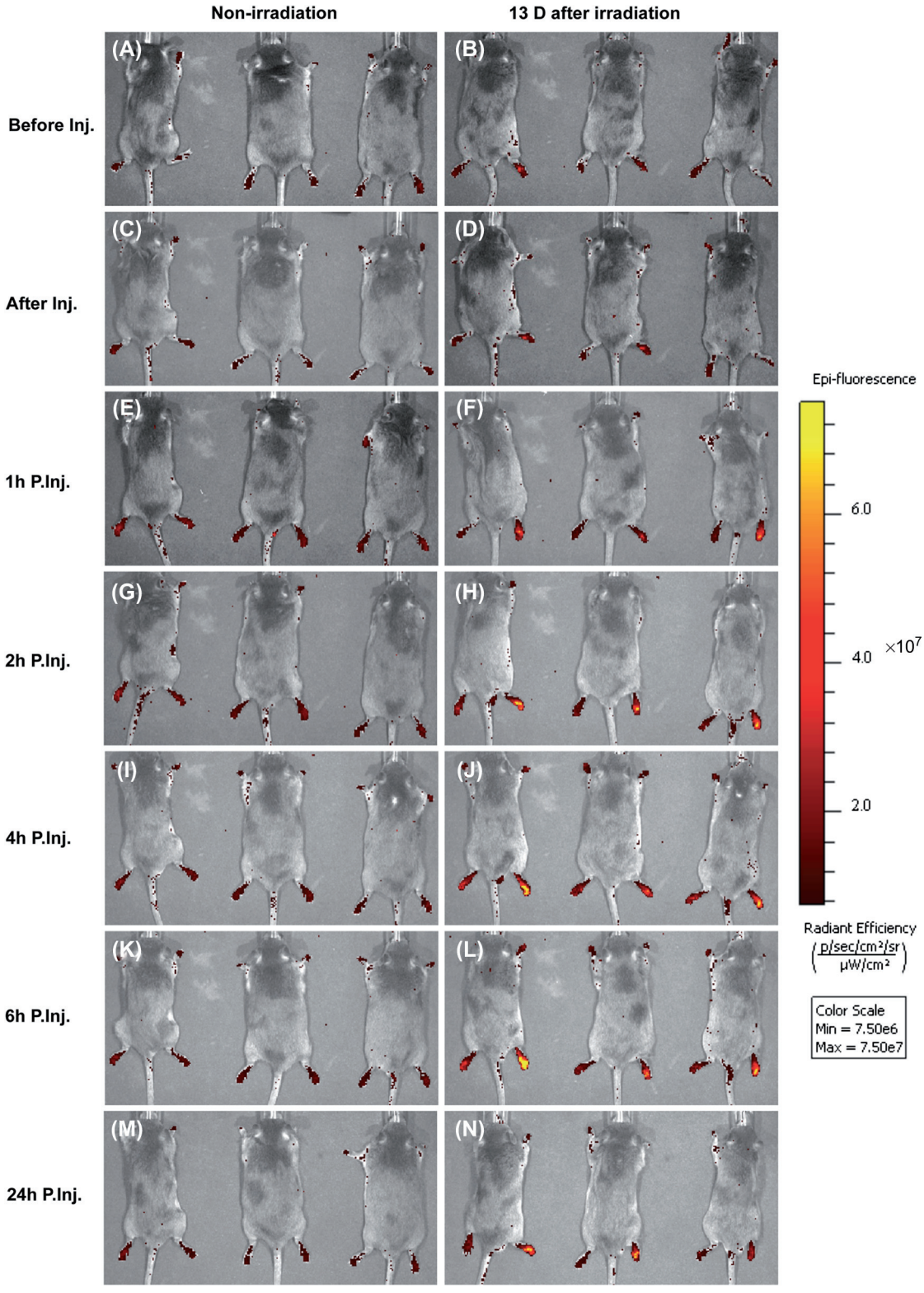

Figure 2. Optical fluorescence imaging of chitosan/Cy5 siRNA nanoparticles in a murine radiation-induced fibrosis model. Mice irradiated 13 days before imaging or without irradiation (Control) (n = 5) were administrated i.p. with chitosan/Cy5 labeled siRNA nanoparticles. Fluorescent optical imaging was performed at distinct time points after injection of fluorescently labeled siRNA/chitosan particles. A, C, E, G, I, K, M and B, D, F, H, J, L, N represent images of three mice from the control group without irradiation and the irradiated group (irradiated 13 days before imaging). Images were taken before and right after injection of chitosan/Cy5-siRNA, as well as one, two, four, six, 24 hours post-injection, respectively.

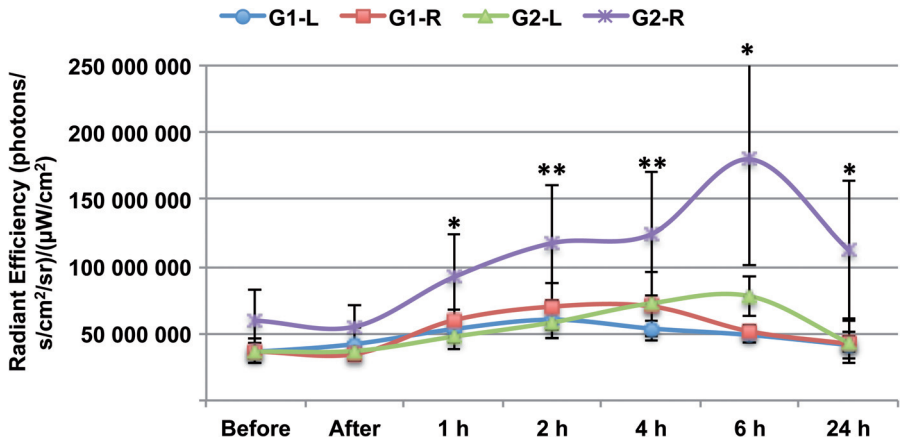

Figure 3. Quantification of the fluorescence signals from the footpads. To quantify the signal intensity of images from Figure 2, the radiant efficiency [(photons/s/cm^2/sr)/(μW/cm^2)] was measured using Living Image 4.0 software package. The average value of left and right footpads from each group was presented (mean ± SD, n = 5). Student t-test was performed to compare the signal between right and left footpads in irradiated mice, '*' p-value < 0.05 and '**' p-value < 0.01. G1 represents control group for mice without irradiation and G2 represents irradiated group for mice irradiated at right hind leg/paws with dose of 45 Gy for 13 days. L and R represent left and right footpads from each group, respectively. G1-L, G1-R and G2-L were non-irradiated footpads.

genetic modifications of macrophages to express reporter genes ex vivo.

In the former method, macrophages are readily labeled ex vivo due to their intrinsic capacity to internalize foreign particles with no need for cell surface modification. After reinjection into the animal cell, migration can be tracked using non-invasive techniques like MRI, PET or optical imaging. MRI in combination with the administration of iron oxide or gadolinium (Gd)-based particles has been applied in inflammatory disease models of atherosclerosis and myocardial infraction [10,11], rheumatoid arthritis [12,13] and in brain inflammation models [14,15]. Contrast signal detected in the lesion region by MRI and iron oxide particle uptake in the macrophages could be confirmed by histological analysis

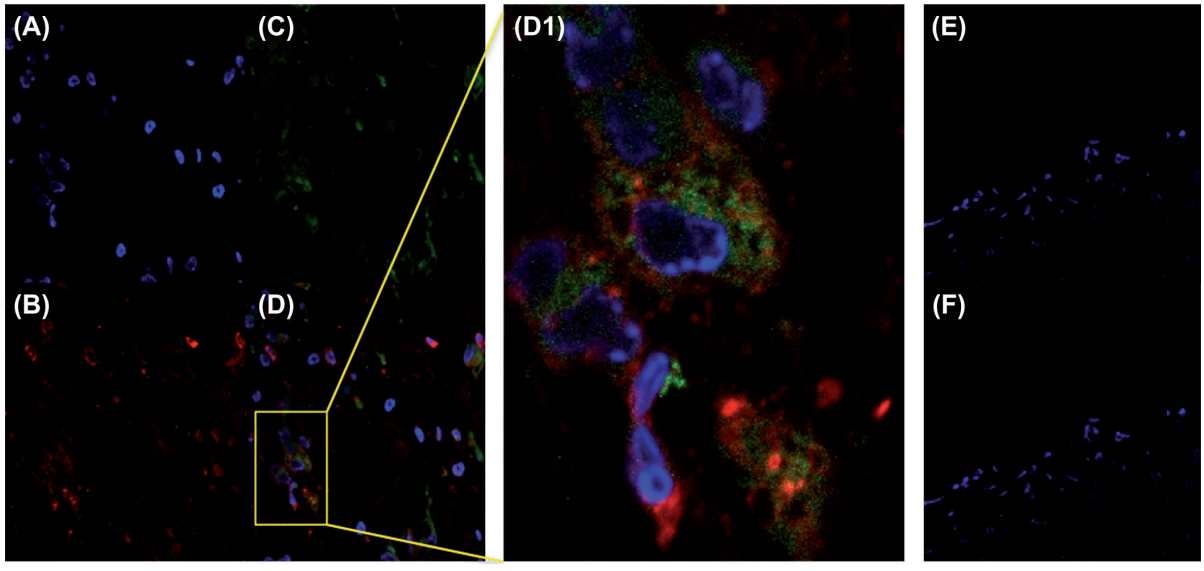

Figure 4. Co-localization of chitosan/Cy3 labeled siRNA nanoparticles and peritoneal macrophages in the irradiated skin of the hind leg. Male mice were irradiated with a dose of 45 Gy or left without irradiation as a control. After 13 days chitosan/Cy3 labeled siRNA nanoparticles were administrated i.p.. Four hours later skin samples were taken from irradiated and non-irradiated leg/paws. These were stained for F4/80, a macrophage marker and examined by confocal laser microscopy. Represented pictures from irradiated tissue are shown as A–D, Cy3 signal (Green) was only observed within F4/80 positive cells (Red), whereas non-irradiated skin did not show signal for Cy3 (E&F, and not shown). D1 represented the enlarged image in selected region (rectangle) from the D. As there was no signal for both macrophage staining and Cy3 fluorescence in non-irradiated skin, they were not shown. Therefore the merge (F) showed same pattern to DAPI one (E). A and E, nuclei are stained using DAPI (Blue); B, macrophages are immunohistochemically stained using F4/80; C, Cy3 signal from siRNA; D and F, pictures are merged.

in some studies. PET has the advantage of high sensitivity but relative poor resolution and is often combined with molecular-genetic imaging strategies [6]. In the latter method, genetic imaging strategies are based on imaging the product from continuously expressed reporters within cells in the body [6]. One example used the sodium/iodide symporter (NIS) reporter gene combined with radiotracers such as radio-iodine to monitor the RAW264.7 EGFP/NIS expressing macrophage cell line migration toward a chemically induced inflammation lesion [7]. The study demonstrated an intense signal at the lesion site by PET after intravenous administration of stably transfected cells, and both NIS and GFP expressed macrophages could be detected at the lesion tissues by immunochemistry. Similar results were obtained using RAW264.7 with a bioluminescent reporter gene being detected by bioluminescence in vivo [16].

A potential problem with genetic modification of macrophages is the introduction of recombinant genetic constructs that may influence the cellular metabolism. In addition, it is generally difficult to obtain high expression of transgenes in macrophages, which limits the applicability of this approach. Similarly, administration of fluorescent particles, magnetic particles or other nanostructures may also influence cellular behavior. One study suggested the migration of peripheral monocytes toward the inflammatory lesion site through the detection of the enhancement signal by MRI after injection of free particles [17], but only few studies apply this strategy for tracking peritoneal macrophages [18,19] and no studies to our knowledge describe the migration of macrophages in connection with radiation-induced fibrosis.

In our study the fluorescent signal from chitosan/Cy5 labeled siRNA nanoparticles was only evident in the leg irradiated with a dose of 45 Gy 13 days before the imaging but not in either the non-irradiated leg in the same mouse, or in mice receiving the same dose but only one, four or eight days post-radiation imaging. The result suggested that the accumulation of nanoparticles require the onset of the acute phase of radiation-induced fibrosis, usually occurring 10–12 days after radiation. One possibility is that activated monocytes and macrophages produce pro-inflammatory cytokines such as IL-6, IL-1 and TNF-α, which in turn will attract other macrophages and lymphocytes. In addition, activated macrophages and stimulated stromal cells synthesize fibrogenic cytokines such as TGF-β [20,21], which suggests that inflammation is implicated in fibrosis and plays an initiating role [22]. However, there are controversial reports, i.e. that the fibrogenetic mechanisms are distinct from inflammatory factors and inflammation may be needed to reverse established and progressive fibrosis [23,24].

The results from us and others further imply that the role of distant macrophages is different from the local macrophages as demonstrated in a recent report [25] where it was found that lung macrophages probably were not involved in the early inflammatory phase of bleomycin-induced lung fibrosis, but rather during the subsequent progressive fibrotic phase [25]. Our result supports a model where migration of activated peritoneal macrophages to inflamed sites occurs extremely fast, less than one hour post-administration of the nanoparticles and can be retained at the site for at least for 24 hours. This host macrophage trafficking was much faster than observed for ex vivo labeled or genetic modified macrophages where migration was observed over two to seven days [7,16].

To investigate the possibility that the chitosan/Cy5 labeled siRNA nanoparticles migrated alone to the inflamed site, we examined the association of the chitosan/Cy3 labeled siRNA nanoparticles with peritoneal macrophages in the irradiated leg. Again, we only observed an intracellular Cy3 signal in irradiated skin whereas no signal was detected in non-irradiated skin. Furthermore, the cellular co-localization of the Cy3 signal and murine macrophage specific F4/80 antibody strongly suggests that the chitosan/Cy3 labeled siRNA was carried by macrophages into the inflammatory tissue.

It is often argued whether macrophages accumulating in inflamed tissue originate from a distant migration (classically activated M1) or recruited from the resident tissue (alternatively activated M2) [26]. In a mouse-human chimera SCID mouse model fluorescently labeled human blood monocytes were systemically administrated and analyzed [27]. Here it was demonstrated that macrophages in pre-transplanted peri-prosthetic tissue were specifically of human origin identified by immunohistochemical staining, indicating the importance of the distantly recruited macrophages. However, the loss of T or B cell function in SCID mice may influence their conclusion. In a tumor model study it was also demonstrated that the uptake of a magneto-optical imaging probe PG-GD-NIR813 was associated with CD68 (pan macrophage marker) and CD169 (classically activated macrophage M1 marker) signals, but not with CD163 (M2 alternatively activated macrophage marker) [28]. However, controversial findings still leave this question open. It was suggested that self-renewed resident macrophages contributed to local accumulation more efficiently than the recruited distant macrophages during T helper 2 (TH2)-related inflammatory pathologies [29]. Also a phenotype shift between M1 and M2 cannot be excluded since a comprehensive study in a lung fibrosis

model recently demonstrated that circulating 'inflammatory' macrophages could promote resident macrophages switching to be alternatively activated [25].

To further understand the role of macrophages during inflammation and fibrosis, as well as their uptake and activity of drugs, staining with specific antibodies for resident macrophages, e.g. CD163, will be helpful. Depletion of macrophages locally or systemically could be an alternative approach. It has been shown that macrophage depletion can enhance fibrosis [28], which may result from a retarded ECM degradation due to lack of macrophage [30]. The macrophage depletion strategy could be applied in our future studies, to elucidate the mechanism for anti-inflammatory and anti-fibrotic nanoparticle-based therapies, although there are controversial reports for the role of inflammation in progressive fibrosis [23,24].

In conclusion, we provide evidence for a model where peritoneal macrophage take up nanoparticles and traffic them to the lesion region in murine radiation-induced skin inflammation. This work will contribute to further development of macrophage mediated RNAi as a therapeutic strategy to combat inflammatory diseases.

Acknowledgements

This project was supported by 'The Lundbeck Foundation Nanomedicine Centre for Individualized Management of Tissue Damage and Regeneration' (LUNA), 'The Lundbeck Foundation Centre for Interventional Research in Radiation Oncology' (CIRRO), the Danish Council for Strategic Research, and the Danish Cancer Society. We thank Dr. San Hein for chitosan preparation, Dr. Daniel M. Dupont for discussion of Living Image, Inger Marie Horsman and Dorthe Grand for their excellent technical assistance.

Declaration of interest: The authors report no conflicts of interest. The authors alone are responsible for the content and writing of the paper.

References

[1] Beckmann N, Cannet C, Babin AL, Ble FX, Zurbruegg S, Kneuer R, et al. In vivo visualization of macrophage infiltration and activity in inflammation using magnetic resonance imaging. Wiley Interdiscip Rev Nanomed Nanobiotechnol 2009;1:272–98.

[2] Howard KA, Rahbek UL, Liu X, Damgaard CK, Glud SZ, Andersen MO, et al. RNA interference in vitro and in vivo using a novel chitosan/siRNA nanoparticle system. Mol Ther 2006;14:476–84.

[3] Nawroth I, Alsner J, Behlke MA, Besenbacher F, Overgaard J, Howard KA, et al. Intraperitoneal administration of chitosan/DsiRNA nanoparticles targeting TNFalpha prevents radiation-induced fibrosis. Radiother Oncol 2010;97:143–8.

[4] Howard KA, Paludan SR, Behlke MA, Besenbacher F, Deleuran B, Kjems J. Chitosan/siRNA nanoparticle-mediated TNF-alpha knockdown in peritoneal macrophages for anti-inflammatory treatment in a murine arthritis model. Mol Ther 2009;17:162–8.

[5] Takanashi M, Oikawa K, Sudo K, Tanaka M, Fujita K, Ishikawa A, et al. Therapeutic silencing of an endogenous gene by siRNA cream in an arthritis model mouse. Gene Ther 2009;16:982–9.

[6] Serganova I, Blasberg R. Reporter gene imaging: Potential impact on therapy. Nucl Med Biol 2005;32:763–80.

[7] Seo JH, Jeon YH, Lee YJ, Yoon GS, Won DI, Ha JH, et al. Trafficking macrophage migration using reporter gene imaging with human sodium iodide symporter in animal models of inflammation. J Nucl Med 2010;51:1637–43.

[8] Paulos CM, Turk MJ, Breur GJ, Low PS. Folate receptor-mediated targeting of therapeutic and imaging agents to activated macrophages in rheumatoid arthritis. Adv Drug Deliv Rev 2004;56:1205–17.

[9] Stone HB. Leg contracture in mice: An assay of normal tissue response. Int J Radiat Oncol Biol Phys 1984;10:1053–61.

[10] Herborn CU, Vogt FM, Lauenstein TC, Dirsch O, Corot C, Robert P, et al. Magnetic resonance imaging of experimental atherosclerotic plaque: Comparison of two ultrasmall superparamagnetic particles of iron oxide. J Magn Reson Imaging 2006;24:388–93.

[11] Amirbekian V, Lipinski MJ, Briley-Saebo KC, Amirbekian S, Aguinaldo JG, Weinreb DB, et al. Detecting and assessing macrophages in vivo to evaluate atherosclerosis noninvasively using molecular MRI. Proc Natl Acad Sci USA 2007;104:961–6.

[12] Beckmann N, Kneuer R, Gremlich HU, Karmouty-Quintana H, Ble FX, Muller M. In vivo mouse imaging and spectroscopy in drug discovery. NMR Biomed 2007;20:154–85.

[13] Saborowski O, Simon GH, Raatschen HJ, Wendland MF, Fu Y, Henning T, et al. MR imaging of antigen-induced arthritis with a new, folate receptor-targeted contrast agent. Contrast Media Mol Imaging 2007;2:72–81.

[14] Wiart M, Davoust N, Pialat JB, Desestret V, Moucharrafie S, Cho TH, et al. MRI monitoring of neuroinflammation in mouse focal ischemia. Stroke 2007;38:131–7.

[15] Saleh A, Schroeter M, Jonkmanns C, Hartung HP, Modder U, Jander S. In vivo MRI of brain inflammation in human ischaemic stroke. Brain 2004;127:1670–7.

[16] Ren PG, Lee SW, Biswal S, Goodman SB. Systemic trafficking of macrophages induced by bone cement particles in nude mice. Biomaterials 2008;29:4760–5.

[17] Oude Engberink RD, Blezer EL, Hoff EI, van der Pol SM, van der Toorn A, Dijkhuizen RM, et al. MRI of monocyte infiltration in an animal model of neuroinflammation using SPIO-labeled monocytes or free USPIO. J Cereb Blood Flow Metab 2008;28:841–51.

[18] Rosen H, Gordon S. Adoptive transfer of fluorescence-labeled cells shows that resident peritoneal macrophages are able to migrate into specialized lymphoid organs and inflammatory sites in the mouse. Eur J Immunol 1990;20:1251–8.

[19] Bellingan GJ, Caldwell H, Howie SE, Dransfield I, Haslett C. In vivo fate of the inflammatory macrophage during the resolution of inflammation: Inflammatory macrophages do not die locally, but emigrate to the draining lymph nodes. J Immunol 1996;157:2577–85.

[20] Haase O, Rodemann HP. Fibrosis and cytokine mechanisms: Relevant in hadron therapy? Radiother Oncol 2004;73(Suppl 2):S144–7.

[21] Bentzen SM. Preventing or reducing late side effects of radiation therapy: Radiobiology meets molecular pathology. Nat Rev Cancer 2006;6:702–13.

[22] Yarnold J, Brotons MC. Pathogenetic mechanisms in radiation fibrosis. Radiother Oncol 2010;97:149–61.
[23] Wynn TA. Cellular and molecular mechanisms of fibrosis. J Pathol 2008;214:199–210.
[24] Wynn TA, Barron L. Macrophages: Master regulators of inflammation and fibrosis. Semin Liver Dis 2010;30:245–57.
[25] Gibbons MA, Mackinnon AC, Ramachandran P, Dhaliwal K, Duffin R, Phythian-Adams AT, et al. Ly6Chi monocytes direct alternatively activated pro-fibrotic macrophage regulation of lung fibrosis. Am J Respir Crit Care Med 2011;184:569–81.
[26] Hume DA. The mononuclear phagocyte system. Curr Opin Immunol 2006;18:49–53.
[27] Zhang K, Jia TH, McQueen D, Gong WM, Markel DC, Wooley PH, et al. Circulating blood monocytes traffic to and participate in the periprosthetic tissue inflammation. Inflamm Res 2009;58:837–44.
[28] Melancon MP, Lu W, Huang Q, Thapa P, Zhou D, Ng C, et al. Targeted imaging of tumor-associated M2 macrophages using a macromolecular contrast agent PG-Gd-NIR813. Biomaterials 2010;31:6567–73.
[29] Jenkins SJ, Ruckerl D, Cook PC, Jones LH, Finkelman FD, van RN, et al. Local macrophage proliferation, rather than recruitment from the blood, is a signature of TH2 inflammation. Science 2011;332:1284–8.
[30] Duffield JS, Forbes SJ, Constandinou CM, Clay S, Partolina M, Vuthoori S, et al. Selective depletion of macrophages reveals distinct, opposing roles during liver injury and repair. J Clin Invest 2005;115:56–65.

Supplementary material available online

Supplementary Figure 1.